

Spatial and Temporal Variability of Vegetation Indices with Industrial Tomato Yield

Marcos Paulo de O. Martins¹, Elton F. dos Reis¹ & Luana de L. Lopes²

¹ Agricultural Engineering Department, State University of Goiás, Anápolis, Goiás, Brazil

² Institute of Agrarian Sciences, Federal University of Uberlândia, Uberlândia, Minas Gerais, Brazil

Correspondence: Marcos Paulo de O. Martins, Agricultural Engineering Department, State University of Goiás, Anápolis, Goiás, 75132-903, Brazil. E-mail: marcospmartins.92@gmail.com

Received: September 16, 2023

Accepted: October 23, 2023

Online Published: October 31, 2023

doi:10.5539/jsd.v16n6p42

URL: <https://doi.org/10.5539/jsd.v16n6p42>

Abstract

Vegetation indices indicate crop development and help identify areas with potential productivity reduction in the desired crop. Thus, this study aimed to determine the spatial and temporal influence of vegetation indices on industrial tomato (*Solanum lycopersicum* L.) yield. The research was conducted at Barcelos Farm in Anápolis, GO, covering a 55-hectare area. A sampling grid of 61-point pairs, spaced at 90 x 90 meters, was established using a GPS receiver. Vegetation indices were characterized by measuring the Soil Plant Analysis Development (SPAD) index, foliar nitrogen content through the Kjeldahl method, and Normalized Difference Vegetation Index (NDVI) using both a spectroradiometer and satellite imagery. Industrial tomato yield was assessed during harvest. Through the results, it was observed that temporal variability between vegetation indices and actual foliar nitrogen content exhibited a significant and positive correlation with industrial tomato productivity, particularly during the flowering stage. However, temporal variability between vegetation indices and foliar nitrogen content displayed low correlation across the mapped areas over time. Determining foliar nitrogen content and vegetation indices during the flowering stage is recommended for the industrial tomato crop. The relationship between ground-based remote sensing NDVI and orbital NDVI displayed a 55% positive correlation during the flowering stage.

Keywords: foliar nitrogen, georeferencing, precision agriculture, remote sensing, *Solanum lycopersicum* L.

1. Introduction

Tomatoes (*Solanum lycopersicum* L.) are a widely cultivated crop and one of the most consumed vegetables due to their nutritional value, particularly the antioxidant compounds lycopene and carotenoid, which have been associated with health benefits (Colanero et al., 2020; Martí et al., 2016; Mozos et al., 2018; Sousa et al., 2020).

Crop yield can vary across seasons, locations, and even within the same field due to management practices and environmental conditions (Kayad et al., 2022). Monitoring this variability is crucial for farmers, landowners, and insurers to make informed decisions (Kayad et al., 2022; Oliveira et al., 2018). Soil, as a key factor in agricultural production, exhibits considerable variability in tropical regions, with diverse physical and chemical characteristics that influence crop growth and productivity (Amorim et al., 2022). Spatial and temporal variability of soil properties significantly impact crop yield, making it important to understand this variation and its relationship with crop performance for precision management practices (Kayode et al., 2022; Zhou et al., 2020).

Precision agriculture offers technologies to manage field variability (Finkenbiner et al., 2019), with geotechnologies such as remote sensing proving to be powerful tools for this purpose (Medorio-García et al., 2020; Wang et al., 2019). Through remote sensing, imagery is acquired and analyzed using specific algorithms to generate suitable information layers for decision-making and optimizing input rates (Kayad et al., 2022). Geostatistical methods enable the quantification of spatial variation, revealing the spatial structure, randomness, and correlation of samples, facilitating spatially irregular sampling for optimal interpolation (Zhou et al., 2020).

The chlorophyll content is an indicator of vegetation photosynthesis, which directly influences the growth and yield of crops, and is therefore an indicator of their health (Yuan et al., 2022). The SPAD (Soil Plant Analysis Development) chlorophyll meter has been widely used to quickly analyze the status of chlorophyll and nitrogen in leaves, indirectly estimates the chlorophyll concentration in a time-saving non-destructive way (Mehrabi & Sepaskhah, 2022). Leaf chlorophyll content can also be determined by the destructive method of solvent extraction

in the laboratory.

The Normalized Difference Vegetation Index (NDVI), derived from multispectral images, is an effective indicator for assessing vegetation status and quantified attributes. Remote sensing images provide composite images for subsequent interpretation and analysis (Huang et al., 2021). According to Barros et al. (2020), NDVI is relevant because it can provide a view of the condition of vegetation, through images generated by remote sensors, usually satellites, drones or ground sensors. Furthermore, if the NDVI values are well below the expected value, it shows that there is an anomaly that must be checked. Chen et al. (2021) describe that NDVI data derived from Landsat satellites are pertinent resources for vegetation monitoring. Understanding what may be occurring is a precondition for developing effective strategies for greater productivity. Big data availability in agriculture, supported by free remote sensing data and sensor-based information, offers opportunities to understand field variability and implement site-specific precision agriculture practices (Toscano et al., 2019).

Considering the aforementioned, this study aims to evaluate the influence of spatial and temporal variability of vegetation indices on industrial tomato yield. It seeks to establish relationships between field-measured nitrogen content, remotely sensed vegetation indices, and the comparison of ground-based and orbital NDVI for industrial tomato cultivation.

2. Materials and Methods

2.1 Experimental Area Location and Characterization

The study was carried out at the Barcelos Farm in the city of Anápolis, Goiás State, Brazil. It lies at an average altitude of 995 m and geographical coordinates of 16° 25' 57.62" South latitude and 48° 50' 29.61" West longitude. According to the Köppen classification system, the region has an Aw type climate (i.e., Tropical Rainforest Climate).

The area has a low-slope topography, and the soil is classified as a Dark Red Latosol with a clayey-loamy texture (Teixeira et al., 2017).

The industrial tomato crop, cultivar NS 901, was established on a 55-ha area (Figure 1), irrigated using a center pivot system. The seedlings were transplanted in single rows with a spacing of 1.0 m between rows and 0.36 m between plants, resulting in a population density of 36,000 plants ha⁻¹.

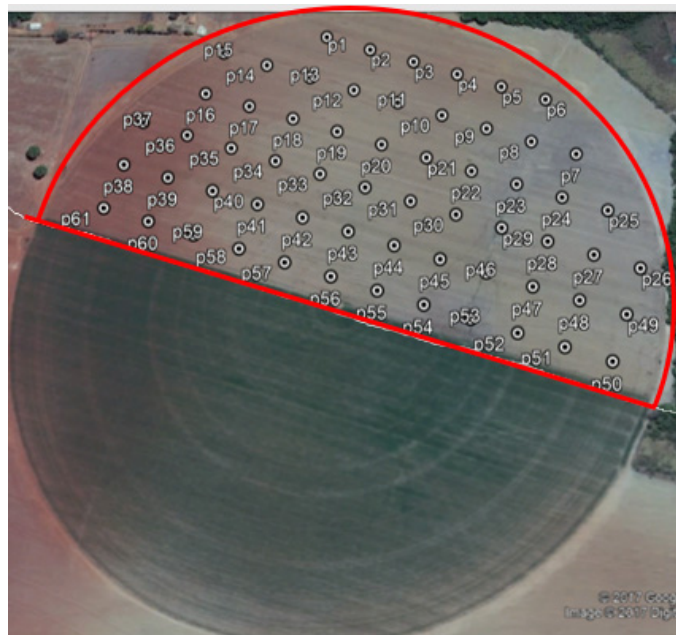


Figure 1. Representative image of the industrial tomato production area

Note. The area enclosed in the highlighted semicircle represents the satellite image of the industrial tomato production area at Barcelos Farm with georeferenced points. Source: Google Earth, 2018.

The area was fertilized before seedling transplanting with 1100 kg ha⁻¹ of 04-30-16 N-P-K formulation. Top-dressings were performed with 150 kg ha⁻¹ potassium chloride (KCl), 170 kg ha⁻¹ ammonium sulfate (NH₄)₂SO₄

and 5 kg ha⁻¹ potassium nitrate (KNO₃), split into three applications.

2.2 Georeferencing of the Area

Before planting, a sampling grid was established using a Garmin ETREX global positioning system (GPS) device with geographic coordinates (GSW84), and geographic coordinates were collected at the ends and center of the pivot, defining the arrangement of the sampling grid. The area was composed of a sampling grid with 61 georeferenced points spaced at 90 x 90 m intervals (Figure 1).

2.3 Data Collection

Crop vegetation indexes were collected 37, 53, and 69 days after transplanting (DAT). It was aligned with the satellite overpasses and intervals of nitrogen top-dressing (16 days). Industrial tomato yield data were collected at the harvest point (108 DAT) in August of the 2017 crop season. The data were collected at each georeferenced point.

2.4 Determination of Crop Vegetation Indexes

2.4.1 Soil Plant Analysis Development (SPAD) Index

The Soil Plant Analysis Development (SPAD) index was determined by taking three readings using a portable chlorophyll meter (ClorofiLOG® model CFL 1030), which provides total chlorophyll values with the Falker Chlorophyll Index (FCI). At each sampling grid point, the SPAD index value comprised the average of readings taken on ten leaves from ten industrial tomato plants. The readings were taken on the central region of leaves in the upper third of the plants between 10:00 a.m. and 2:00 p.m. (Fontes & Araújo, 2007; Singh et al., 2017).

2.4.2 Laboratory Determination of Foliar Nitrogen (FN) Content in Industrial Tomatoes

Foliar nitrogen (FN) contents were determined on the same ten leaves used for SPAD. After SPAD determination, the leaves were removed from each plant, stored in pre-labeled plastic bags, and sent to the analytical chemistry laboratory at the State University of Goiás to determine the NF concentration.

The samples were dried in a forced-air oven at 75 ± 3°C until reaching a constant weight (four and a half hours). Then, the samples were ground using a Wiley-type mill with a 0.5 mm sieve, and a fraction of 0.5 g of the dried samples was weighed. For NF extraction, the samples were analyzed using the micro-Kjeldahl method (Kjeldahl, 1883).

After the NF extraction process, the calculation was performed to obtain the percentage of total nitrogen present in the leaf (Badr et al., 2016; MAPA, 2013; Souza et al., 2014), according to Equation 1.

$$\% \text{ TN} = \frac{V \times N \times 0.014 \times 100}{M} \quad (1)$$

In which:

%TN – percentage of total nitrogen;

V - milliliters of 0.1 mol L⁻¹ HCl solution used in titration;

N - theoretical normality of 0.1 mol L⁻¹ hydrochloric acid solution;

M - mass of the sample in grams.

The FN content analysis was performed 37, 53, and 69 DAT of the tomato seedlings.

2.4.3 Acquisition of Radiometric Data for Industrial Tomato Crop

Radiometric readings were obtained using a spectroradiometer with a passive sensor from Ocean Optics, model USB 2000+RAD. The device was used to obtain reflectance data within the spectral range of 400 to 900 nm at a 0.34 nm resolution. It was connected to a portable computer, where the data were stored. The device was installed on a metallic support, maintaining a height of 1 m above the crop canopy (Singh et al., 2017).

For this study, the values of reflectance corresponding to the wavelengths of Landsat 8 satellite bands were used. The values from Band 4, red (640-690 nm), and Band 5, near-infrared (850-880 nm) were used to determine the vegetation indices, specifically the Normalized Difference Vegetation Index (NDVI) (Rouse et al., 1974; Zanzarini et al., 2013), according to Equation 2.

$$\text{NDVI} = \frac{\text{IR} - \text{R}}{\text{IR} + \text{R}} \quad (2)$$

In which:

NDVI - Normalized Difference Vegetation Index;

IR - average value of near-infrared reflectance in Band 4;

R - average value of red reflectance in Band 3.

The reflectance values were obtained as the average of three readings taken around each sample point within a 1.5 m radius. The readings were taken between 10:00 a.m. and 2:00 p.m. due to the consistent solar radiation. The readings were performed 37, 53, and 69 DAT of the tomato seedlings.

2.4.4 Remote Sensing of Industrial Tomato

Remote sensing was performed by acquiring Landsat 8 satellite images corresponding to the days 06/05/2017 (37 DAT), 06/21/2017 (53 DAT), and 07/06/2017 (69 DAT), with a 16-day interval following the satellite overpass days. After the acquisition, the images were obtained from the National Institute for Space Research (INPE), and using the QGIS software, vegetation indices were calculated using the Normalized Difference Vegetation Index (NDVI) as the variable (Rouse et al., 1974; Zanzarini et al., 2013), according to Equation 3.

$$NDVI = \frac{B5 - B4}{B5 + B4} \quad (3)$$

In which:

NDVI = Normalized Difference Vegetation Index;

B4 = red band;

B5 = near-infrared band.

2.5 Productivity of Industrial Tomato Crop

The yield of industrial tomato crop was evaluated at the harvest time (108 DAT) in August of the 2017 crop season. At each georeferenced point of the sampling grid, a representative 1-m² area was demarcated around the point, and all fruits within the demarcated area were collected. The collected fruits were weighed using a calibrated portable digital scale (Marine-type fisherman scale) with a precision of 0.01 g and a maximum capacity of 40 kg. After weighing, the sample weights were extrapolated to t ha⁻¹ for all sampled points (Figueiredo et al., 2016).

2.6 Data Analysis

2.6.1 Descriptive Statistics

Exploratory data analysis was conducted to identify outliers and assess the statistical distribution of the vegetation indices and industrial tomato productivity data. The critical limit for outliers was defined based on the interquartile range (IQR), calculated as the difference between the upper quartile (Q3) and the lower quartile (Q1). The upper limit for outliers was defined as (Q3 + 1.5 × IQR), and the lower limit as (Q1 - 1.5 × IQR), where Q1 and Q3 are the first and third quartiles, respectively, according to the methodology adjusted by Bottega et al. (2013).

Descriptive statistics were calculated using spreadsheet software, including the mean, median, minimum value, maximum value, coefficient of variation, standard deviation, skewness, and kurtosis, to analyze the distribution of the data (Burak et al., 2016). The coefficient of variation (CV) was classified as low (CV < 12%), medium (12% ≤ CV ≤ 60%), and high (CV > 60%), following the classification adapted by Ferreira Júnior et al. (2021).

2.6.2 Pearson's Correlation

Pearson's correlation analysis was conducted by creating a correlation matrix, and simple linear correlations (r) were calculated using spreadsheet software. The attribute combinations were evaluated in pairs, and correlations were interpreted according to a classification adapted by Bermudez-Edo et al. (2018): null correlation (0.0 < r < 0.1), weak correlation (0.1 < r < 0.3), moderate correlation (0.3 < r < 0.5), strong correlation (0.5 < r < 0.8), and very strong correlation (0.8 < r < 1.0).

2.6.3 Geostatistical Analysis

To characterize spatial variability, geostatistical analysis was performed, where each evaluated attribute was analyzed individually to identify spatial dependence through calculation of simple semivariograms. The semivariograms were fitted based on the assumption of intrinsic hypothesis (Usovicz & Lipiec, 2017).

The mathematical model for the fitted semivariograms was selected based on the lowest sum of squared residuals (RSS), highest coefficient of determination (r²), and greatest degree of spatial dependence (SDD), according to Monteiro et al. (2017).

The mathematical model of the fitted semivariograms for each attribute provided the parameters for nugget effect

(C0), structural variance (C1), sill (C0 + C1), and range (A). The degree of spatial dependence (SDD) was analyzed based on the relationship between the structural variance and the sill. SDD was interpreted as follows: very low dependence (SDD < 20%), low dependence (20% < SDD < 40%), moderate dependence (40% < SDD < 60%), high dependence (60% < SDD < 80%), and very high dependence (80% < SDD < 100%) (Dalchiavon & Carvalho, 2012).

The semivariogram models for the studied variables were fitted using GS+ software, version 7. Once the spatial dependence of the studied variables was confirmed, ordinary kriging interpolation was used to estimate values at unmeasured locations, and thematic maps were built using Surfer 8 software.

3. Results and Discussion

According to descriptive statistics (Table 1), the different vegetation indices and productivity showed similar mean and median values, indicating a normal distribution of the data. This is supported by the skewness coefficients, which ranged from -0.68 to 0.54, indicating a low deviation from the mean.

Table 1. Descriptive statistics of vegetation indices and yield of industrial tomato crop

Variable	Mean	Med.	Min.	Max.	SD	Kurt.	Asymm.	CV (%)
SPAD_1	428.82	427.90	400.60	472.10	16.17	-0.14	0.34	3.77
SPAD_2	427.91	427.50	381.20	469.20	18.47	-0.24	-0.10	4.32
SPAD_3	411.81	413.60	347.90	483.50	30.45	-0.23	-0.18	7.39
FN_1	5.67	5.78	4.37	6.84	0.62	-0.44	-0.23	10.90
FN_2	5.41	5.40	4.57	6.23	0.40	-0.21	0.08	7.33
FN_3	4.40	4.30	3.00	5.60	0.55	-0.26	0.30	12.40
NDVI_Es_1	0.80	0.82	0.70	0.88	0.04	-0.40	-0.68	5.50
NDVI_Es_2	0.78	0.78	0.69	0.84	0.03	-0.73	-0.44	4.46
NDVI_Es_3	0.65	0.65	0.55	0.75	0.05	-0.51	0.11	7.75
NDVI_St_1	0.48	0.48	0.41	0.53	0.03	-0.51	-0.41	5.81
NDVI_St_2	0.45	0.45	0.39	0.50	0.02	-0.54	-0.22	5.48
NDVI_St_3	0.41	0.40	0.36	0.47	0.02	-0.19	0.21	5.80
Yield	80.00	77.40	61.00	108.80	12.14	-0.31	0.54	15.22

Note. SPAD_1=Soil plant analysis development index; FN_1=Foliar nitrogen; NDVI_Es_1=Spectroradiometer-based vegetation index; NDVI_St_1=Satellite-based vegetation index; SPAD_2=Soil plant analysis development index; FN_2=Foliar nitrogen; NDVI_Es_2=Spectroradiometer-based vegetation index; NDVI_St_2=Satellite-based vegetation index; SPAD_3=Soil plant analysis development index; FN_3=Foliar nitrogen; NDVI_Es_3=Spectroradiometer-based vegetation index; NDVI_St_3=Satellite-based vegetation index; Med.=Median; Min.=Minimum; Max.=Maximum; SD=Standard deviation; Kurt.= Kurtosis; Asymm.=Asymmetry; CV (%)=Coefficient of Variation.

The variables exhibited negative kurtosis coefficients, ranging from -0.14 to -0.73, implying data flattening compared to the normal curve. The Soil Plant Analysis Development Index (SPAD), Foliar Nitrogen (FN) at the flowering stage (53 DAT), and Satellite-based Normalized Difference Vegetation Index (NDVI) at the early fruit formation stage (69 DAT) displayed a mesokurtic normal distribution. The remaining variables throughout the crop cycle exhibited a leptokurtic normal distribution. According to Sanquetta et al. (2014), kurtosis values below -0.263 and between -0.263 to 0.263 define a leptokurtic and mesokurtic normal distribution, respectively.

The coefficients of variation (CV) were classified following Ferreira Júnior et al. (2021). The vegetation indices variables were categorized as low CV when values were below 12%, while industrial tomato productivity was classified as medium with a value exceeding 12%. Similar results were found by Padilla et al. (2017) for vegetation indices in cucumber crops.

Foliar nitrogen content serves as an indicator of photosynthetic protein quantity and plays a significant role in understanding plant functioning and status (Jia et al., 2021). Foliar nitrogen analysis revealed mean values of

5.67%, 5.41%, and 4.40% at 37, 53, and 69 DAT, respectively, representing the nitrogen percentage (N) in the leaves of industrial tomato plants. Cheng et al. (2022) also observed a decrease in nitrogen concentration in cherry tomato plants as the growth period progressed. In the 2019 season, nitrogen concentration in plants ranged from 2.2%, 1.58%, to 1.44% at 34, 48, and 77 DAT, respectively. Lequeue et al. (2016) reported an average nitrogen content of 1.71% in tomato leaves.

The readings obtained for industrial tomato NDVI using a spectroradiometer showed mean values of 0.80, 0.78, and 0.65 at 37, 53, and 69 DAT, respectively, which aligns with the findings of Marino et al. (2014) and Fortes Gallego et al. (2015). Avotins et al. (2020) studied the NDVI for 6 tomato cultivars at different plant heights, and observed that the values varied between 0.667 and 0.871. The results that the authors found show potential application in crop management by monitoring the quality parameters of tomato plant growth.

Regarding NDVI calculated from Landsat 8 satellite imagery for industrial tomato, the mean values were 0.48, 0.45, and 0.41 at 37, 53, and 69 DAT, respectively. Lykhovyd et al. (2022) observed an increase in average NDVI values for tomato crops from planting (0.17) to the fruit formation stage (0.69), followed by a decrease to 0.45 during fruit ripening. Maselli et al. (2020) observed, in tomato cultivation areas, an increase in NDVI (up to 0.7) until the moment of maximum biomass development. These findings were based on satellite imagery.

Vegetation indices displayed a reduction in nitrogen levels throughout the crop's development stages, particularly after 69 DAT, during the early fruit formation stage. According to Ronga et al. (2015), this stage corresponds to an increased nutrient demand by the plant. Guo et al. (2020) describe studies that showed that the concentration of N in crops reduces with increasing biomass.

The average productivity of industrial tomatoes was 80.0 t ha⁻¹. While these values were higher than those reported by Fortes Gallego et al. (2015) (66.0 t ha⁻¹), they were comparable to the findings of Oliveira et al. (2018) (82.7 t ha⁻¹) for the same crop.

Simple linear correlation analysis using Pearson's correlation coefficient (r) was employed to determine the correlation between productivity and vegetation indices of industrial tomatoes (Table 2).

Table 2. Pearson's correlation analysis (r) of vegetation indices and yield of industrial tomato crop

Variable	SPAD_1	SPAD_2	SPAD_3	FN_1	FN_2	FN_3	NDVI_Es_1	NDVI_Es_2	NDVI_Es_3	NDVI_St_1	NDVI_St_2	NDVI_St_3	Productivity
SPAD_1	1.000												
SPAD_2	-0.242	1.000											
SPAD_3	0.127	-0.155	1.00										
FN_1	-0.188	-0.101	-0.115	1.00									
FN_2	-0.143	0.265 *	0.077	0.060	1.00								
FN_3	-0.226	-0.039	-0.001	-0.006	-0.137	1.00							
NDVI_Es_1	0.241	0.127	-0.013	-0.111	0.257 *	-0.337 *	1.00						
NDVI_Es_2	0.251	-0.039	0.054	-0.240	0.044	-0.193	0.375 *	1.00					
NDVI_Es_3	0.129	-0.102	-0.01	-0.098	0.264 *	-0.124	0.308 *	0.731 *	1.000				
NDVI_St_1	0.395 *	-0.128	-0.039	-0.307 *	-0.123	-0.329 *	0.454 *	0.350 *	0.147	1.000			
NDVI_St_2	0.401 *	-0.198	-0.013	-0.186	0.088	-0.275 *	0.349 *	0.551 *	0.603 *	0.648 *	1.000		
NDVI_St_3	0.376 *	-0.301 *	0.008	-0.171	0.060	-0.182	0.204	0.560 *	0.704 *	0.439 *	0.856 *	1.000	
Yield	0.131	-0.106	-0.139	-0.025	0.180	0.039	0.123	0.266 *	0.245	0.106	0.169	0.235	1.000

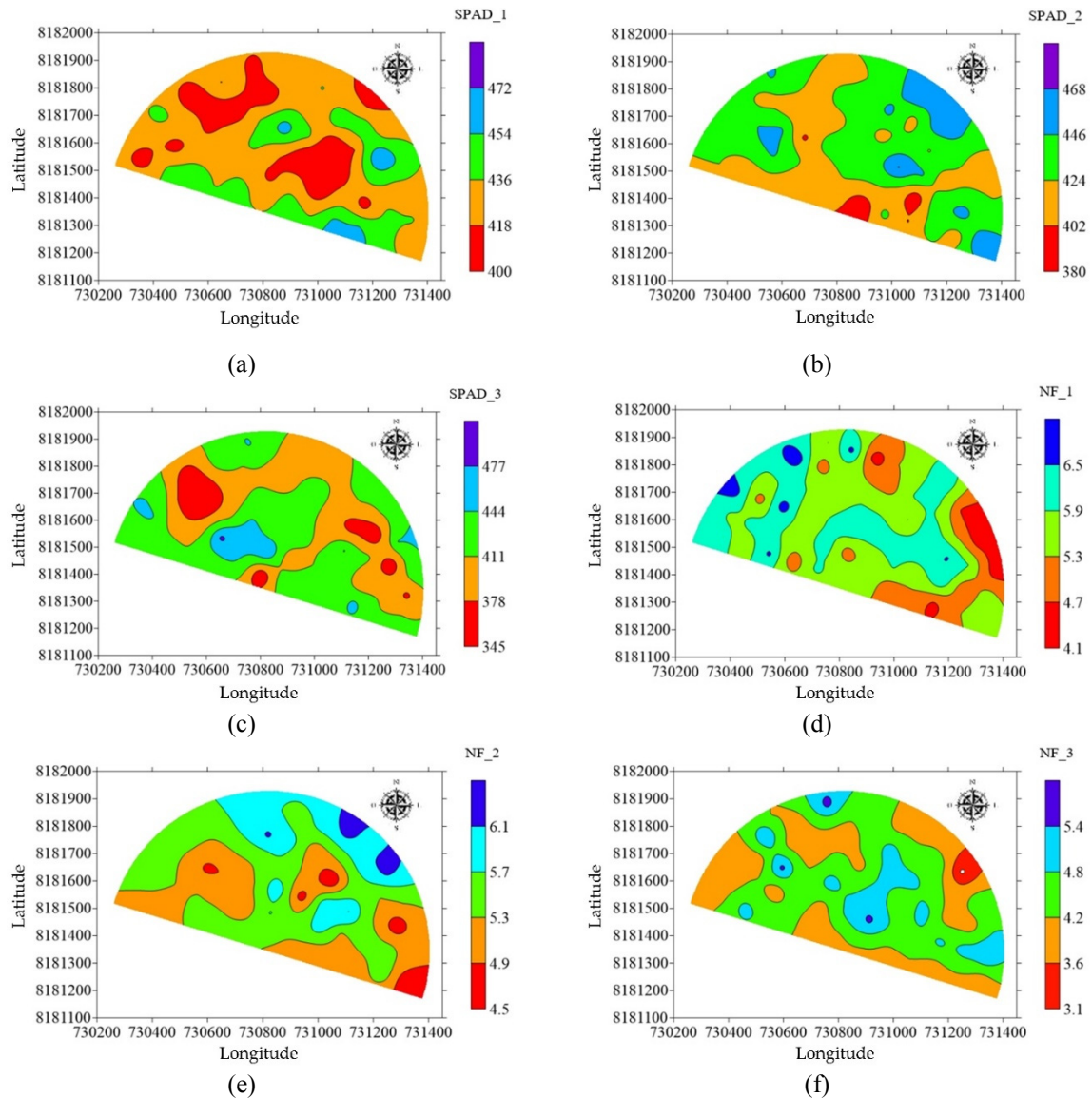
Note. SPAD_1=Soil plant analysis development index; FN_1=Foliar nitrogen; NDVI_Es_1=Spectroradiometer-based vegetation index; NDVI_St_1=Satellite-based vegetation index; SPAD_2=Soil plant analysis development index; FN_2=Foliar nitrogen; NDVI_Es_2=Spectroradiometer-based vegetation index; NDVI_St_2=Satellite-based vegetation index; SPAD_3=Soil plant analysis development index; FN_3=Foliar nitrogen; NDVI_Es_3=Spectroradiometer-based vegetation index; NDVI_St_3=Satellite-based vegetation index; *significant at 5% probability.

The Spectroradiometer-based Vegetation Index at 37 DAT (NDVI_Es_1) showed a moderate, positive, and

significant correlation with NDVI_St_1 (0.454*). At 53 DAT, NDVI_Es_2 displayed a strong, positive, and significant correlation with NDVI_St_2 (0.551*), indicating a higher nitrogen concentration for vegetative development that can influence crop productivity. The readings at 69 DAT (NDVI_Es_3) and NDVI_St_3 exhibited a strong, positive, and significant correlation (0.704*).

The NDVI_Es and NDVI_St readings showed a strong, positive, and significant correlations throughout the crop cycle, indicating that both readings by through ground-based and orbital remote sensing images are significant to diagnose crop development. The wavelength reflectance for ground-based NDVI measurements in industrial tomatoes aligns with the values reported by Marino et al. (2014) and Fortes Gallego et al. (2015).

The spatial maps of vegetation indices and industrial tomato yield were generated using spherical semivariogram parameters, which had better fit by kriging interpolation to estimate values in unsampled locations for characterizing spatial dependency (Figure 2).



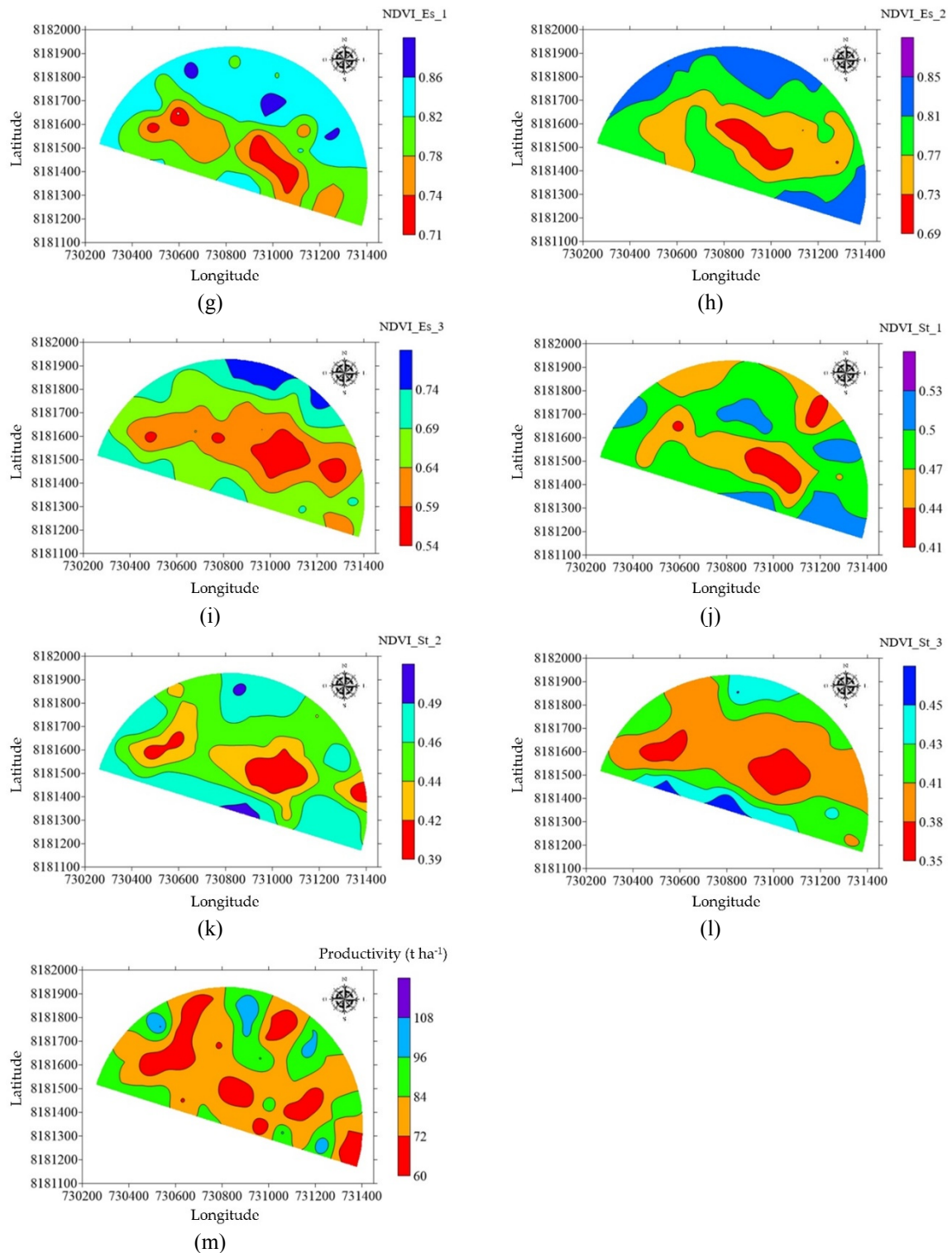


Figure 2. Contour maps

Note. (a) SPAD_1=Soil plant analysis development index; (b) SPAD_2=Soil plant analysis development index; (c) SPAD_3=Soil plant analysis development index; (d) FN_1=Foliar nitrogen; (e) FN_2=Foliar nitrogen; (f) FN_3=Foliar nitrogen; (g) NDVI_Es_1=Spectroradiometer-based vegetation index; (h) NDVI_Es_2=Spectroradiometer-based vegetation index; (i) NDVI_Es_3=Spectroradiometer-based vegetation index; (j) NDVI_St_1=Satellite-based vegetation index; (k) NDVI_St_2=Satellite-based vegetation index; (l) NDVI_St_3=Satellite-based vegetation index; (m) Industrial tomato yield.

The maps of vegetation indices showed little variation throughout the industrial tomato crop cycle. The first reading at 37 DAT (Figure 2A) revealed that the southern, central, and northeastern regions exhibited higher SPAD index variation, with small areas ranging from 436 to 472, higher than in other regions. Figure 2D illustrates the spatial distribution of FN content in the crop, highlighting the southeastern region with low nitrogen content ranging from 4.1% to 5.3%, while the southwestern and central-western regions had FN content exceeding 5.9%.

The NDVI readings at 37 DAT using ground-based and orbital remote sensing are shown in Figures 2G and 2J, respectively. Both methods identified low NDVI values in the southwestern and central-western regions, ranging from 0.70 to 0.78 for NDVI_Es and from 0.41 to 0.47 for NDVI_St.

At the second vegetation index reading during the flowering stage (53 DAT), there was a prevalence of low SPAD index in the northwest, south, and southeast regions, ranging from 380 to 424 (Figure 2B). Other regions showed an increase in the SPAD index due to the second nitrogen top-dressing application. Figure 2E characterizes the spatial dependency of FN content, revealing low FN content in the southwestern, part of central-western, and southeastern regions, ranging from 4.5% to 5.3%. A small area in the southeastern region showed even lower FN content.

The NDVI readings at 53 DAT exhibited less spatial dependency in the western, central, and eastern regions, as shown in Figures 2H and 2K for ground-based and satellite-based measurements, respectively. These maps (Figures 2H and 2K) illustrate the central region's greater NDVI reduction between 37 and 53 DAT.

For the third vegetation index reading at 69 DAT, during the early fruit formation stage, the SPAD index map (Figure 2C) indicates that the western, northern, and southeastern regions exhibited lower values, ranging from 345 to 411. The spatial dependency of FN content (Figure 2F) featured higher values of 4.2% to 5.4% in the western, northern, central-western, and southeastern regions, while other regions had lower values than 4.2%.

The NDVI maps obtained from spectroradiometer and satellite imagery readings are represented by Figures 2I and 2L, respectively, with the central region showing lower NDVI values due to nitrogen fertilization in the industrial tomato crop, ranging from 0.54 to 0.64 and 0.35 to 0.41, respectively.

The NDVI maps of the different crop stages highlight the similarity among the regions and a strong correlation between spectroradiometer and satellite imagery readings (Table 2). The maps revealed a strong spatial dependency of the evaluated vegetation indices in the northern region. These results enable the characterization of management zones and the identification of regions that may influence crop development.

The readings across the different crop stages showed the spatial and temporal variability of vegetation indices in industrial tomatoes. The maps revealed a strong spatial dependency of the evaluated vegetation indices in the northern region. These results enable the characterization of management zones and identification of regions that may influence crop development.

The yield map of industrial tomatoes (Figure 2M) highlights the southwestern, northern, and northeastern regions as those with higher yields (from 84 to 108 t ha⁻¹). When correlated with all vegetation index maps, we noted that the regions with higher yields also had better vegetation indices for crop development. Table 2 showed a correlation between yield and vegetation indices during the flowering stage of the crop (53 DAT). Overall, regions with higher yields also had higher vegetation indices.

4. Conclusions

The spatial variability of vegetation indices, foliar nitrogen content, and industrial tomato yield can be determined.

The temporal variability between vegetation indices and foliar nitrogen content indicates that the highest correlation with tomato industrial yield is reached at the flowering stage.

The correlation between vegetation index maps and crop yield allows us to identify regions with higher productivity potential.

Regions with lower normalized difference vegetation indices (NDVIs) coincide with reduced industrial tomato yields. Additionally, there is a positive correlation of 55% between NDVI obtained through terrestrial and orbital remote sensing during the flowering stage of the tomato crop.

Temporal variability between vegetation indices and foliar nitrogen content shows low correlation across the developmental cycle of the crop.

Based on the obtained results, we recommend determining foliar nitrogen content and vegetation indices during the flowering stage of the industrial tomato crop.

References

- Amorim, M. T. A., Silvero, N. E. Q., Bellinaso, H., Gómez, A. M. R., Greschuk, L. T., Campos, L. R., & Demattê, J. A. M. (2022). Impact of soil types on sugarcane development monitored over time by remote sensing. *Precision Agriculture, 23*(5), 1532–1552. <https://doi.org/10.1007/s11119-022-09896-1>
- Avotins, A., Kvišis, K., Bicans, J., Alsina, I., & Dubova, L. (2020). Experimental analysis of IoT based camera SI-NDVI values for tomato plant health monitoring application. *Agronomy Research, 18*(S2), 1138–1146. <https://doi.org/10.15159/AR.20.087>
- Badr, M. A., Abou-Hussein, S. D., & El-Tohamy, W. A. (2016). Tomato yield, nitrogen uptake and water use efficiency as affected by planting geometry and level of nitrogen in an arid region. *Agricultural Water Management, 169*, 90–97. <https://doi.org/10.1016/j.agwat.2016.02.012>
- Barros, A. S., de Farias, L. M., & Marinho, J. L. A. (2020). Aplicação do Índice de Vegetação por Diferença Normalizada (NDVI) na Caracterização da Cobertura Vegetativa de Juazeiro Do Norte-CE. *Revista Brasileira de Geografia Física, 13*(6), 2885–2895.
- Bermudez-Edo, M., Barnaghi, P., & Moessner, K. (2018). Analysing real world data streams with spatio-temporal correlations: Entropy vs. Pearson correlation. *Automation in Construction, 88*, 87–100. <https://doi.org/10.1016/j.autcon.2017.12.036>
- Bottega, E. L., Pinto, F. de A. de C., Queiroz, D. M. de, Santos, N. T., & Souza, C. M. A. de. (2013). Variabilidade espacial e temporal da produtividade de soja no Cerrado brasileiro. *Agrarian, 6*(20), Article 20.
- Burak, D. L., Santos, D. A., & Passos, R. R. (2016). Variabilidade espacial de atributos físicos: Relação com relevo, matéria orgânica e produtividade em café conilon. *Coffee Science, 11*(4), 455–466. <http://www.sbicafe.ufv.br/handle/123456789/8240>
- Chen, Y., Cao, R., Chen, J., Liu, L., & Matsushita, B. (2021). A practical approach to reconstruct high-quality Landsat NDVI time-series data by gap filling and the Savitzky–Golay filter. *ISPRS Journal of Photogrammetry and Remote Sensing, 180*, 174–190. <https://doi.org/10.1016/j.isprsjprs.2021.08.015>
- Cheng, M., He, J., Wang, H., Fan, J., Xiang, Y., Liu, X., Liao, Z., Tang, Z., Abdelghany, A. E., & Zhang, F. (2022). Establishing critical nitrogen dilution curves based on leaf area index and aboveground biomass for greenhouse cherry tomato: A Bayesian analysis. *European Journal of Agronomy, 141*, 126615. <https://doi.org/10.1016/j.eja.2022.126615>
- Colanero, S., Perata, P., & Gonzali, S. (2020). What’s behind Purple Tomatoes? Insight into the Mechanisms of Anthocyanin Synthesis in Tomato Fruits. *Plant Physiology, 182*(4), 1841–1853. <https://doi.org/10.1104/pp.19.01530>
- Dalchiavon, F. C., & Carvalho, M. de P. e. (2012). Correlação linear e espacial dos componentes de produção e produtividade da soja. *Semina: Ciências Agrárias, 33*(2). <https://doi.org/10.5433/1679-0359.2012v33n2p541>
- Ferreira Júnior, O. J., Santos, A. C. dos, Naves Júnior, C. H., Mendes, F. C., Ramalho, T. A. de Q., Sousa, W. L. de, Teixeira, M. M., Aguiar, G. R., & Flor, M. V. C. (2021). Spatial distribution of soil chemical properties in the cerrado of Tocantins. *Revista Engenharia na Agricultura - REVENG, 29*(Continua), 335–346. <https://doi.org/10.13083/reveng.v29i1.11908>
- Figueiredo, A. S., Resende, J. T., Faria, M. V., Paula, J. T., Rizzardi, D. A., & Meert, L. (2016). Agronomic evaluation and combining ability of tomato inbred lines selected for the industrial segment. *Horticultura Brasileira, 34*, 86–92. <https://doi.org/10.1590/S0102-053620160000100013>
- Finkenbiner, C. E., Franz, T. E., Gibson, J., Heeren, D. M., & Luck, J. (2019). Integration of hydrogeophysical datasets and empirical orthogonal functions for improved irrigation water management. *Precision Agriculture, 20*(1), 78–100. <https://doi.org/10.1007/s11119-018-9582-5>
- Fontes, P. C. R., & Araújo, C. de. (2007). *Aducação nitrogenada de hortaliças: Princípios e práticas com o tomateiro*. Viçosa, MG: UFV.
- Fortes Gallego, R., Prieto Losada, M. del H., García Martín, A., Córdoba Pérez, A., Martínez, L., & Campillo Torres, C. (2015). Using NDVI and guided sampling to develop yield prediction maps of processing tomato crop. *Spanish Journal of Agricultural Research, 13*(1), e0204. <https://doi.org/10.5424/sjar/2015131-6532>
- Guo, Q., Zhu, Y., Tang, Y., Hou, C., He, Y., Zhuang, J., Zheng, Y., & Luo, S. (2020). CFD simulation and experimental verification of the spatial and temporal distributions of the downwash airflow of a quad-rotor agricultural UAV in hover. *Computers and Electronics in Agriculture, 172*, 105343.

- <https://doi.org/10.1016/j.compag.2020.105343>
- Huang, S., Tang, L., Hupy, J. P., Wang, Y., & Shao, G. (2021). A commentary review on the use of normalized difference vegetation index (NDVI) in the era of popular remote sensing. *Journal of Forestry Research*, 32(1), 1–6. <https://doi.org/10.1007/s11676-020-01155-1>
- Jia, M., Colombo, R., Rossini, M., Celesti, M., Zhu, J., Cogliati, S., Cheng, T., Tian, Y., Zhu, Y., Cao, W., & Yao, X. (2021). Estimation of leaf nitrogen content and photosynthetic nitrogen use efficiency in wheat using sun-induced chlorophyll fluorescence at the leaf and canopy scales. *European Journal of Agronomy*, 122, 126192. <https://doi.org/10.1016/j.eja.2020.126192>
- Kayad, A., Rodrigues, F. A., Naranjo, S., Sozzi, M., Pirotti, F., Marinello, F., Schulthess, U., Defourny, P., Gerard, B., & Weiss, M. (2022). Radiative transfer model inversion using high-resolution hyperspectral airborne imagery – Retrieving maize LAI to access biomass and grain yield. *Field Crops Research*, 282, 108449. <https://doi.org/10.1016/j.fcr.2022.108449>
- Kayode, O. T., Aizebeokhai, A. P., & Odukoya, A. M. (2022). Geophysical and contamination assessment of soil spatial variability for sustainable precision agriculture in Omu-Aran farm, Northcentral Nigeria. *Heliyon*, 8(2), e08976. <https://doi.org/10.1016/j.heliyon.2022.e08976>
- Kjeldahl, J. (1883). A new method for the determination of nitrogen in organic matter. *Zeitschrift für Analytische Chemie*, 22, 366–382. <http://dx.doi.org/10.1007/BF01338151>
- Lequeue, G., Draye, X., & Baeten, V. (2016). Determination by near infrared microscopy of the nitrogen and carbon content of tomato (*Solanum lycopersicum* L.) leaf powder. *Scientific Reports*, 6(1). <https://doi.org/10.1038/srep33183>
- Likhovyd, P., Vozhehova, R., & Lavrenko, S. (2022). Annual NDVI dynamics observed in industrial tomato grown in the south of Ukraine. *Mod. Phytomorphol*, 16, 164–169.
- MAPA, M. D. A., PECUÁRIA E. ABASTECIMENTO. (2013). *Determinação de nitrogênio total em leite e derivados lácteos pelo método de micro-kjedahl*, 2-8. <http://www.agricultura.gov.br/assuntos/laboratorios/legislacoes-e-metodos/arquivos-metodos-da-area-poa-iaq/met-poa-11-02-proteinas.pdf>
- Marino, S., Aria, M., Basso, B., Leone, A. P., & Alvino, A. (2014). Use of soil and vegetation spectroradiometry to investigate crop water use efficiency of a drip irrigated tomato. *European Journal of Agronomy*, 59, 67–77. <https://doi.org/10.1016/j.eja.2014.05.012>
- Martí, R., Roselló, S., & Cebolla-Cornejo, J. (2016). Tomato as a Source of Carotenoids and Polyphenols Targeted to Cancer Prevention. *Cancers*, 8(6). <https://doi.org/10.3390/cancers8060058>
- Maselli, F., Angeli, L., Battista, P., Fibbi, L., Gardin, L., Magno, R., Rapi, B., & Chiesi, M. (2020). Evaluation of Terra/Aqua MODIS and Sentinel-2 MSI NDVI data for predicting actual evapotranspiration in Mediterranean regions. *International Journal of Remote Sensing*, 41(14), 5186–5205. <https://doi.org/10.1080/01431161.2020.1731000>
- Medorio-García, H. P., Alarcón, E., Flores-Esteves, N., Montañón, N. M., & Perroni, Y. (2020). Soil carbon, nitrogen and phosphorus dynamics in sugarcane plantations converted from tropical dry forest. *Applied Soil Ecology*, 154, 103600. <https://doi.org/10.1016/j.apsoil.2020.103600>
- Mehrabi, F., & Sepaskhah, A. R. (2022). Leaf Nitrogen, Based on SPAD Chlorophyll Reading Can Determine Agronomic Parameters of Winter Wheat. *International Journal of Plant Production*, 16(1), 77–91. <https://doi.org/10.1007/s42106-021-00172-2>
- Monteiro, A., Menezes, R., & Silva, M. E. (2017). Modelling spatio-temporal data with multiple seasonalities: The NO2 Portuguese case. *Spatial Statistics*, 22, 371–387. <https://doi.org/10.1016/j.spasta.2017.04.005>
- Mozos, I., Stoian, D., Caraba, A., Malainer, C., Horbańczuk, J. O., & Atanasov, A. G. (2018). Lycopene and Vascular Health. *Frontiers in Pharmacology*, 9. Retrieved from <https://www.frontiersin.org/articles/10.3389/fphar.2018.00521>
- Oliveira, D. G. de, Reis, E. F. dos, Medeiros, J. C., Martins, M. P. de O., & Umbelino, A. da S. (2018). Correlation indices physical space of soil and productivity of fruit tomato industry. *Agro@ambiente On-line*, 12(1), 1–10.
- Padilla, F. M., Peña-Fleitas, M. T., Gallardo, M., & Thompson, R. B. (2017). Determination of sufficiency values of canopy reflectance vegetation indices for maximum growth and yield of cucumber. *European Journal of Agronomy*, 84, 1–15. <https://doi.org/10.1016/j.eja.2016.12.007>

- Ronga, D., Lovelli, S., Zaccardelli, M., Perrone, D., Ulrici, A., Francia, E., Milc, J., & Pecchioni, N. (2015). Physiological responses of processing tomato in organic and conventional Mediterranean cropping systems. *Scientia Horticulturae*, *190*, 161–172. <https://doi.org/10.1016/j.scienta.2015.04.027>
- Rouse, J. W., Haas, R. H., Schell, J. A., & Deering, D. W. (1974). Monitoring vegetation systems in the Great Plains with ERTS. *NASA Spec. Publ.*, *351*(1), 309.
- Sanquetta, C. R., Behling, A., Corte, A. P. D., Ruza, M. S., Simon, A. A., & José, J. F. B. S. (2014). Relação hipsométrica em inventários pré-corte em povoamentos de *Acacia mearnsii* De Wild. *Científica*, *42*(1), Article 1. <https://doi.org/10.15361/1984-5529.2014v42n1p80-90>
- Singh, S. K., Houx, J. H., Maw, M. J. W., & Fritsch, F. B. (2017). Assessment of growth, leaf N concentration and chlorophyll content of sweet sorghum using canopy reflectance. *Field Crops Research*, *209*, 47–57. <https://doi.org/10.1016/j.fcr.2017.04.009>
- Sousa, B., Lopes, J., Leal, A., Martins, M., Soares, C., Valente, I. M., Rodrigues, J. A., Fidalgo, F., & Teixeira, J. (2020). Response of *Solanum lycopersicum* L. to diclofenac – Impacts on the plant’s antioxidant mechanisms. *Environmental Pollution*, *258*, 113762. <https://doi.org/10.1016/j.envpol.2019.113762>
- Souza, L. C. de, Siqueira, J. A. M., Silva, J. L. de S., Silva, J. N. da, Coelho, C. C. R., Neves, M. G., Oliveira Neto, C. F. de, & Lobato, A. K. da S. (2014). *Compostos nitrogenados, proteínas e aminoácidos em milho sob diferentes níveis de silício e deficiência hídrica*. <http://repositorio.ufra.edu.br/jspui/handle/123456789/523>
- Teixeira, P. C., Donagemma, G. K., Fontana, A., & Teixeira, W. G. (2017). *Manual de métodos de análise de solo*. Brasília: Embrapa.
- Toscano, P., Castrignanò, A., Di Gennaro, S. F., Vonella, A. V., Ventrella, D., & Matese, A. (2019). A Precision Agriculture Approach for Durum Wheat Yield Assessment Using Remote Sensing Data and Yield Mapping. *Agronomy*, *9*(8). <https://doi.org/10.3390/agronomy9080437>
- Usovicz, B., & Lipiec, J. (2017). Spatial variability of soil properties and cereal yield in a cultivated field on sandy soil. *Soil and Tillage Research*, *174*, 241–250. <https://doi.org/10.1016/j.still.2017.07.015>
- Wang, M., Liu, Z., Ali Baig, M. H., Wang, Y., Li, Y., & Chen, Y. (2019). Mapping sugarcane in complex landscapes by integrating multi-temporal Sentinel-2 images and machine learning algorithms. *Land Use Policy*, *88*, 104190. <https://doi.org/10.1016/j.landusepol.2019.104190>
- Yuan, Z., Ye, Y., Wei, L., Yang, X., & Huang, C. (2022). Study on the Optimization of Hyperspectral Characteristic Bands Combined with Monitoring and Visualization of Pepper Leaf SPAD Value. *Sensors*, *22*(1). <https://doi.org/10.3390/s22010183>
- Zanzarini, F. V., Pissarra, T. C. T., Brandão, F. J. C., & Teixeira, D. D. B. (2013). Correlação espacial do índice de vegetação (NDVI) de imagem Landsat/ETM+ com atributos do solo. *Revista Brasileira de Engenharia Agrícola e Ambiental*, *17*, 608–614. <https://doi.org/10.1590/S1415-43662013000600006>
- Zhou, Q., Zhang, B., Jin, J., & Li, F. (2020). Production limits analysis of rain-fed maize on the basis of spatial variability of soil factors in North China. *Precision Agriculture*, *21*(6), 1187–1208. <https://doi.org/10.1007/s11119-020-09714-6>

Acknowledgments

Not applicable

Authors contributions

Conceptualization, M.P.d.O.M., L.d.L.L., and E.F.d.R.; methodology, M.P.d.O.M., L.d.L.L., and E.F.d.R.; software, M.P.d.O.M.; formal analysis, M.P.d.O.M., L.d.L.L., and E.F.d.R.; writing—review and editing, M.P.d.O.M., L.d.L.L., and E.F.d.R.; supervision E.F.d.R., All the authors have read and agreed to the published version of the manuscript.

Funding

Recurso financeiro proveniente da Convocatória n. 21/2022, Termo de Fomento nº 000036040537, Processo SEI n. 202200020020855, Universidade Estadual de Goiás and Coordination for the Improvement of Higher Education Personnel – Brazil (CAPES)

Competing interests

The authors declare that they have no known competing financial interests or personal relationships that could have appeared to influence the work reported in this paper.

Informed consent

Obtained.

Ethics approval

The Publication Ethics Committee of the Canadian Center of Science and Education.

The journal's policies adhere to the Core Practices established by the Committee on Publication Ethics (COPE).

Provenance and peer review

Not commissioned; externally double-blind peer reviewed.

Data availability statement

The data that support the findings of this study are available on request from the corresponding author. The data are not publicly available due to privacy or ethical restrictions.

Data sharing statement

No additional data are available.

Open access

This is an open-access article distributed under the terms and conditions of the Creative Commons Attribution license (<http://creativecommons.org/licenses/by/4.0/>).

Copyrights

Copyright for this article is retained by the author(s), with first publication rights granted to the journal.